Theoretical and Experimental Analysis of OM314 Diesel Engine Combustion and Performance Characteristics Fueled with DME

J. Ghorbanian
MSc. Mechanical Engineering
jafar.ghorbanian@gmail.com

S. A. Jazayeri
Assistant Prof.
Mechanical Engineering Department
K. N. Toosi University of Technology
jazayeri@kntu.ac.ir

L. Savadkouhi
Iranian Research Organization for Science and Technology (IROST)
Tehran, Iran
savadkohi@irost.org

M. Keshavarz *
Iran Heavy Diesel MFG. Co. (DESA)
Amol, Iran
Keshavarz@desa-co.com

* Corresponding Author
Received: Jan. 25, 2007
Accepted in revised form: Sep. 21, 2009

Gh. Javadirad
PhD Candidate
Mechanical Engineering
Babol Noshirvani University of Technology
Javadirad@desa-co.com

S. N. Shahangian
MSc. Mechanical Engineering
Shahangian@desa-co.com

Abstract

Homogeneous Charge Compression Ignition (HCCI) combustion is a pioneer method of combustion in which pre-mixed fuel and oxidizer (typically air) are compressed to the point of auto-ignition. HCCI engines can operate with most alternative fuels, especially, dimethyl ether (DME) which has been tested as a possible diesel fuel due to its simultaneously low NOx and PM emissions. In this paper a single zone detailed chemistry combustion model for determining the time evolution of the homogenous reacting gas mixture in the combustion chamber and performance characteristics of the engine has been developed. The aim of this paper is to analyse the effect of intake temperature and EGR on the characteristics of auto-ignition and operating window of the HCCI combustion considering knock and misfire boundaries.

Keywords: Dimethy Ether, Multi Zone Combustion, Emissions, Disel Engine, Modeling

1. Introduction

There is an interest in improving motor vehicle fuel economy while complying with emissions regulations. Naturally diesel engines have improved fuel economy compared to gasoline vehicles, but it is difficult to control NO_x and particulate matter according to proposed future emissions standards. As modern spark ignition engines operate at stoichiometric conditions, NO_x emissions are controlled by a three-way catalytic converter and particle emissions are low. Since diesel engines operate fuel lean, control of NO_x by a catalyst would be difficult. Diesel particulate emissions are higher than from spark ignition engines and can be reduced via traps, fuel additives, or changes in engine operating strategy.

Several recent publications have presented results from diesel engines or diesel vehicles operated on pure DME [1 and 2]. These experiments showed that DME is an excellent alternative to diesel fuel [3-5] which produces very low particulate and soot emissions. Also the amount of NO_x formation in DME mode operation is less than current diesel engines under the same engine operating conditions.

This allows the engine operating conditions to be adjusted to further reduction of NO_x without an accompanying increase in particulate emissions. DME physical and chemical properties compared with diesel oil are shown in table 1. The properties of DME can be summarized as follows:

• DME has only C-H and C-O bonds without C-C bonds and contains about 34.8% oxygen. Therefore, the combustion produced emissions with DME fuel, such as smoke and PM, are expected to be lower than those using diesel fuels. An engine with DME fuel can tolerate more EGR rate to reduce NO_x [7 and 8].

• The lower heating value of DME is only 64.7% of that of diesel fuel; therefore larger amount of fuel supply per cycle is needed to ensure the same engine power.

• The cetane number of DME is higher than that of diesel fuel and other alternative fuels. Therefore, there is no need for an ignition assisted system as used for methanol, ethanol, and LPG and CNG engines.

• DME is in gaseous state even at -20 °C and ambient pressure. Its Reid vapor pressure varies with the temperature. Therefore, DME needs to be pressurized to over 0.5 MPa to keep it in liquid state under ambient temperature (25°C). The fuel delivery pressure should be increased to 1.7-2.0 MPa under engine operating conditions to prevent from vapor lock in fuel system.

• The latent heat of evaporation of DME is much higher than that of diesel, which is beneficial to the NOx reduction due to lower mixture temperature [8].

The objectives of this study are to investigate the performances and combustion characteristics of a heavy duty truck engine operating on DME. So a quasi steady, multi zone model has been used for performance characteristics and emission production analysis of a heavy duty truck engine powered by DME. The effects of combustion system parameters on engine performances have also been studied.

TABLE 1. Physical and chemical properties of DME and diesel [8]

Properties	DME	Diesel
Chemical formula	CH_3-O-CH_3	C_xH_y
Mole weight, g	46.07	190-220
Boiling point, ˚C	-24.9	180-360
Liquid density, g/cm^3	0.668	0.84
Liquid viscosity, cP	0.15	4.4-5.4
Low heat value/MJ/kg	28-43	42.5
Explosion limit in air,v%	3.4-17	0.6-6.5
Ignition temperature/˚C	235	250
Cetane number	55-60	40-55
Stoichiometric air/fuel ratio, (kg/kg)	9	14.6
%wt of Oxygen	34.6	0
%wt of Carbon	52.2	86

2. Model descriptions

2.1. Assumption

For injection process simulation, following assumptions have been made:

1- Injection zone modeling was done based on Modified Hiroyasu model because of its accuracy and precision. [9]

2- It was assumed that, there is no impingement of the injected fuel into the wall.

As mentioned in the introduction of this paper, the model to be presented is a multi zone one, which means that the resulting jet is divided into discrete volumes, called zones during fuel injection. The number of axial zones is determined by the duration of the fuel injection period and the calculation time step used, while the number of radial zones is determined by making trials and finding the number from which a further increase causes no modification in the model results. In the present study, 80 axial zones and 5 radial zones have been considered for injected spray modeling.

Based on these assumptions, the detailed description of the model is as follows.

2.2. Spray submodel

After the initiation of fuel injection, the zones begin to form and penetrate into the combustion chamber. The Initial conditions at the nozzle exit are obtained from the fuel injection process simulation. The Initial jet velocity is calculated as follows:

$$u_0(t) = \frac{4\dot{m}_f(t)}{n_\circ \pi d_{inj}^2 \rho_1} \quad (1)$$

Where $n_\circ$ and d_{inj} are the number and diameter of the nozzle holes and ρ_1 is the density of the DME.

Similarly to diesel operation, it is supposed that DME fuel initially travels a small distance inside the cylinder before breaking up into droplets. Here, the break up length is computed by the same equation as with diesel operation [9 and 10], but the constant C_1 is much smaller

$$S_b = C_1 \left(\frac{\rho_1}{\rho_a} \right)^{0.5} d_{inj} \quad (2)$$

ρ_a, is surrounding air density.

C_1 is an experimental factor which is related to fuel characteristics.

The velocity along the spray axis is determined by the following equation [9]

$$u_{ij} = \begin{cases} u_0(t_i), & S_{ij} \le S_b \\ u_0(t_i)\left(\dfrac{S_b}{S_{ij}}\right)^{nj}, & S_{ij} > S_b \end{cases} \quad (3)$$

It should be pointed out that t_i in equation (3) represents the moment at which local zone injects into the cylinder.

Concerning the radial velocity component of the zones, the initial value for all zones formed at a given time step is given by the equation

$$u_{ri} = u_\circ \tan\left(\frac{\alpha}{r_\circ} r_i\right) \quad (4)$$

Where $r_\circ$ is the radius of the nozzle hole and r_i is the radial distance of zone i from the center line. The initial spray angle of DME, which is used in equation (4), is obtained from the following relation [10]

$$\alpha = 0.10\left(\frac{d_{inj}^2 \rho_a \Delta p}{\mu_a^2}\right)^{0.25} \quad (5)$$

Where Δp the pressure is difference across the injector hole and μ_a is the dynamic viscosity of the air.

2.3. Mass entrainment submodel

The mass entrainment of zones is calculated on the basis of the momentum conservation principle

$$\frac{dm_z}{dt} = -\frac{m_z}{u_z}\frac{du_z}{dt} \quad (6)$$

Cui et al. [11] show that the air entrainment process in the cylinder is related not only to the fuel injection process but also to the excess air ratio, which means that the mixing takes place between various zones, not just between fresh air and fuel zones. This view is also verified by the experiments. Therefore, the method for calculating mass entrainment presented in reference [11] is adopted in this study. In this method, zones in a cylinder are classified into three groups: the fresh air group, the pollutant gas group and combustion group. Therefore, the combustion zone entrains fresh air and burned gas

$$\frac{dm_{c_i}}{dt} = \frac{dm_{c_i,a}}{dt} + \sum_{j=1}^{J}\frac{dm_{c_i,p_j}}{dt} \quad (7)$$

Where dm_{c_i}/dt is derived from equation (6), and

$$\frac{dm_{c_i,a}}{dt} = \frac{dm_{c_i}}{dt} \times \frac{(1-\eta)m_a}{(1-\eta)m_a + \eta m_p} \quad (8)$$

$$\frac{dm_{c_i,p_j}}{dt} = \frac{dm_{c_i}}{dt} \times \frac{\eta m_{p_j}}{(1-\eta)m_a + \eta m_p} \quad (9)$$

$$m_p = \sum_{j=1}^{J} m_{p_j} \quad (10)$$

Here, η is the coefficient of pollutant entrainment.

The pollutant gas zone p_j entrains fresh air and is entrained by combustion zones

$$\frac{dm_{p_j}}{dt} = \sum_{i=1}^{I}\frac{dm_{p_j,c_i}}{dt} + \frac{dm_{p_i,a}}{dt} \quad (11)$$

where dm_{p_j}/dt is derived from equation (6), and

$$\frac{dm_{p_j,c_i}}{dt} = -\frac{dm_{c_i,p_j}}{dt} \quad (12)$$

The mass change in the fresh air zone can be derived from equations (7) and (11)

$$\frac{dm_a}{dt} = \sum_{i=1}^{I}\frac{dm_{a,c_i}}{dt} + \sum_{j=1}^{J}\frac{dm_{a,p_j}}{dt} \quad (13)$$

The changes in composition and internal energy of each zone that are caused by the mixing between zones can be determined by the same method.

2.4.Heat transfer submodel

Heat transfer to the combustion chamber walls is calculated by Woschni equation

$$\frac{dQ_w}{d\phi} = \frac{1}{6n}\sum_{i=1}^{3}\alpha A_i (T_{Wi} - T) \quad (14)$$

$$\alpha = 265 D^{-0.214}(vP)^{0.786} T^{-0.525} \quad (15)$$

where v shows the piston speed, P is the pressure in the cylinder and the units of D, v, P and T are m, m/s, $10^5 Pa$ and K respectively.

Then, the heat flux is distributed among zones according to the weight factor of each zone

$$\frac{dQ_{z,w}}{dt} = \frac{dQ_w}{dt}\frac{W_z}{\sum_z W_z} \quad (16)$$

2.5. Combustion submodels

After injection of the liquid fuel, fuel jet atomizes into small-sized droplets to enable rapid evaporation. For better understanding the ignition delay, thermodynamic analysis of the fuel droplets is required. Rate of change in the droplet's mass is calculated by:

$$-\frac{dm_{drop}}{dt}=-\frac{d}{dt}\left(\frac{\pi}{6}D^3\rho_F\right)=\frac{\pi}{4}\rho_F\,D\beta \qquad (17)$$

where D shows the droplet diameter, ρ_F is the droplet density and $\beta=-\frac{dD^2}{dt}$ which also can be written as $\beta=\frac{\left(-dA_{drop}/dt\right)}{\pi}$. In this equation $A=\pi D^2$ and β shows the quick evaporation rate of the droplet. Regarding to the fact that, mass flow rate of the fuel by evaporation process on the droplet area can be written as: $m_{F,S}=\frac{\left(-dm_{drop}/dt\right)}{A_{drop}}$

the evaporation rate of the droplet can be written as:

$$\beta=4D\frac{\dot{m}_{F,S}}{\rho} \qquad (18)$$

Because the critical temperature of DME is only 127 °C, which is lower than the compressed-air temperature at the later stage of the compression stroke, the DME injected into the cylinder may vaporize immediately due to the fact that a liquid phase is thermodynamically unstable above the critical temperature. When the temperature of DME is greater than 127 °C, DME becomes a superheated gas and, therefore, no evaporation is associated during mixing. The combustion delay time of the injected fuel is calculated using modified Hiroyasu-Nishida equation [6]:

$$\tau_z=0.003\,P^{-.2.5}\,\phi_z^{1.04}\exp\left(\frac{4000}{T_z}\right) \qquad (19)$$

Burned mass gas is calculated via [12]:

$$\dot{m}_{fb}=\min\left(m_{fv},\frac{m_{az}}{l_0}\right) \qquad (20)$$

The rate of heat release is calculated by:

$$\dot{Q}=H_u\dot{m}_{fb} \qquad (21)$$

3. Modeling of Nitric Oxide formation

The DME operation is very clean, since almost no soot is produced even under heavy loads. However, there is no complete agreement in the literature for nitric oxide, another main pollutant of CI engines. Sorenson et al. reported much lower NO_x with DME [2], whereas Kajitani et al. reported NO_x emissions approximately the same as for diesel fuel operation [4].

In this study extended Zeldovich [12] model has been used for NO_x formation modeling because of its widespread usage and simplicity.

$$N + O_2 \leftrightarrow NO + O$$
$$NO + N \leftrightarrow O + N_2$$
$$OH + N \leftrightarrow NO + H$$

4. Modeling of soot formation

Hiroyasu model has been used for soot formation production [13].

$$\left(\frac{dm_{s,i,j}}{dt}\right)_F=A_f\,(m_{inj,i,j}-m_{d,i,j})\,P^{0.5}\exp\left(\frac{-E_{sf}}{R_u\,T_{i,j}}\right) \qquad (22)$$

where $E_{sf}=1.25\times10^4\ \ kcal/mol$

$m_{s,i,j}$, is soot mass in zone [i,j] and A_f, is constant that are determined by experimental data.

Soot oxidation model investigated in this study is the Nagle and Strickland-Constable oxidation model. The NSC oxidation model is based on oxidation experiments of carbon graphite in an O_2 environment over a range of partial pressure. In this model, carbon oxidation occurs by two mechanisms whose rates oxidation occurs by two mechanisms whose rates A sites and less reactive B sites [14]. The chemical reactions are:

$$A + O_2 \leftrightarrow A + 2CO$$
$$B + O_2 \leftrightarrow A + 2CO$$
$$A \leftrightarrow B$$

The soot oxidation rate will be calculated from:

$$\left(\frac{dm_{s,i,j}}{dt}\right)_O=\frac{MW_C}{\rho_s d_s}m_{s,i,j}w \qquad (23)$$

Therefore

$$\frac{dm_{s,i,j}}{dt}=\left(\frac{dm_{s,i,j}}{dt}\right)_F-\left(\frac{dm_{s,i,j}}{dt}\right)_O \qquad (24)$$

where MW_C, is molecular weight of carbon, ρ_s, is soot density (2.0 g/cm^3), d_s, is soot diameter (4.5 × 10^{-9} m) and w is net reaction rate of proposed reactions mentioned above. This factor is calculated from the method mentioned in [14] and is not presented here.

5. Experimental analysis

In this study the simulation results were validated with experimental results presented in SAE paper [6]. Since in the engine test the indicatory diagram wasn't achieved, the results of another experiment were used to validate the simulated pressure diagram.

The test engine used in this analysis was a water cooled, four cylinder, four stroke naturally aspirated, direct injection diesel engine (Daimler Chrysler motor type, OM314) which is locally produced in I.D.E.M. Co and installed on different models of trucks and buses. The specifications of the engine are shown in table 2. Significant effort was directed at overcoming difficulties with DME leakage in the fuel injection system and at modifying the fuel system to provide the appropriate injection characteristics.

DME is kept in liquid state in the tank in the pressure range of 5-10 bar. Then the fuel pressure is increased up to 300 bar by a geared pump.

TABLE 2. Specifications of the test engine

Cylinder number	4
Piston Bore(mm)	97
Stroke (mm)	128
Compression ratio	17:1
Injection pressure(bar)	250
Nozzle hole diameter, mm	0.3
IVO, IVC	329, -120
EVO,EVC	118, 385
Start of injection	-18

6. Results and discussion

Fig. 1 present a comparison of measured cylinder pressure in reference No. 6, table 3, with calculated ones. As shown, the calculated pressure traces accurately match the measured ones for load examined.

The engine speed is 1600 RPM and for this case only closed cycle, from IVC to EVO, is simulated.

TABLE 3. Specification of engine used in Reference 6

Bore	100 mm	Start of injection	-8 ATDCF
Stroke	115 mm	Fuel amount per cycle	112 mg
Compression Ratio	17.5	Injection shape	Square
Con-Rod length	190 mm	Injection Pressure	250 bar
Pressure @IVC	1.45 bar	Temperature @ IVC	135 oC
Injection start	-8 ATDCF	Injection duration	26 Deg

Fig. 2 shows the results of simulation and engine test. It can be seen that the calculated power error in low speed operation is less than 5% and in high engine speed is approximately 2%.

Fig. 3 shows both the calculated and experimental torque values. Results show that the highest torque in middle range speed can be predicted with less than 4% error. table 4 shows a summary of the results.

Fig. 4 shows the results of volumetric efficiency in different engine speed at WOT. According to the simulation results, maximum value is achieved in middle speed range which consequently gives higher torque values in this operating region. It is worthwhile to mention that reduction in volumetric efficiency in high speed range will cause a proportional reduction in torque values (Figs. 3 and 4).

Considering the accuracy of the simulated results, we have calculated the incylinder pressure, rate of heat released and incylinder temperature in full load and also high torque operations. Figs. 5, 6 and 7 show the pressure, temperature and heat release trajectory respectively for full load and maximum torque operations. Results show 13% pressure rise in the case of full load operation.

TABLE 4. Results of engine torque in different speed range in two cases at WOT

Engine speed	Engine torque (experiment)	Engine torque (simulation)
1300	45.12	47.37
1500	46.55	47.89
1800	47.28	48.393
2200	46.55	47.368
2400	45.35	46.064
2800	40.1	40.854

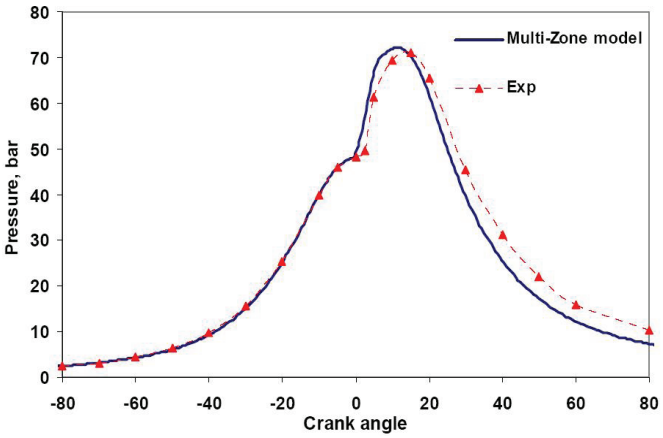

Fig. 1. Comparison of simulation results with experiment

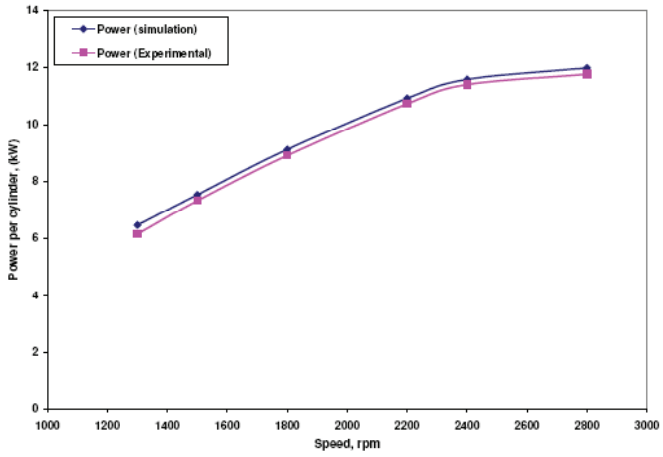

Fig. 2. Comparision of the results of brake power in experiment and simulation

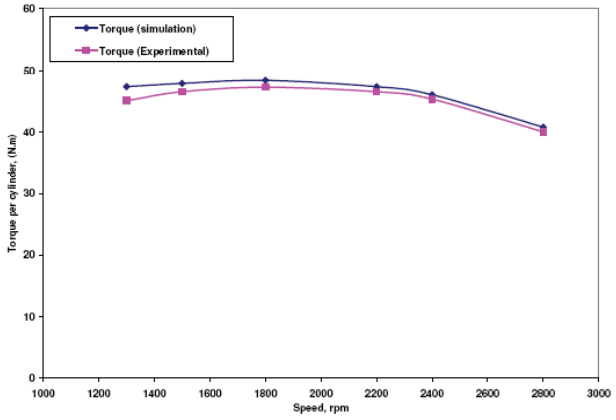

Fig. 3. comparison of the engine brake torque in experiment and simulation

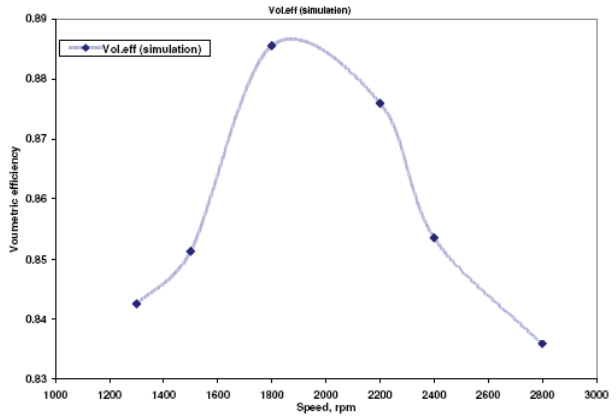

Fig. 4. variation of volumetric efficiency in different engine speed

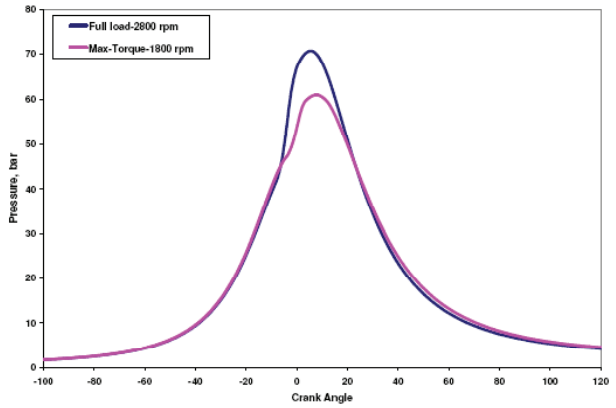

Fig. 5. Comparison of pressure diagram in the case of full load and maximum torque operation

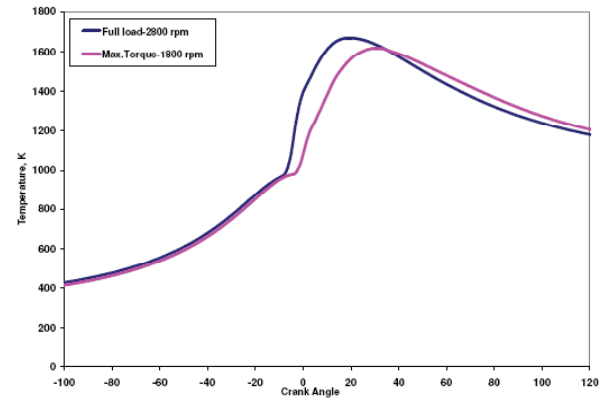

Fig. 6. Comparison of Temperature diagram in the case of full load and maximum torque operation

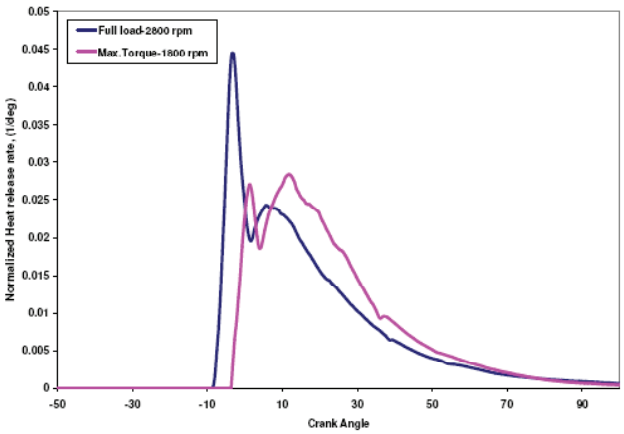

Fig. 7. Comparison of HRR diagram in the case of full load and maximum torque operation

TABLE 5. Results of the maximum Pressure and Temperature in full load and Maximum Torque operation

Simulation results	Maximum Pressure (bar)	Location of Max pressure (ATDC)	Maximum Temperature (K)	Location of Max Temperature (ATDC)
Full load	70.7	5.5	1670	18
Maximum Torque	61	7.74	1617	31

Incylinder pressure in the case of maximum torque has occurred 2 CA earlier respect to full load operation and maximum incylinder temperature has decreased up to 53 °K which shows approximately 5% reduction in this case. As shown in Fig. 7, in full load operation, the portion of premixed heat released is up to 40% higher than maximum torque case which causes higher rate of pressure rise. Figs.s 8 and 9 show a comparison between simulated results of power and torque diagrams for Diesel and DME operation mode in different speed conditions respectively.

It can be clearly seen that in diesel mode operation and in higher speed range (more than 2500 rpm) significant reduction of engine power occurs while in DME mode it is not remarkable. It is also predicted that, in engine speed less than 1900 rpm , maximum power and torque in diesel mode is higher, while in higher speed range (more than 1900 rpm) this would be in the contrary.

Figs. 10 and 11 show the simulated results of brake specific NO_x and Soot in different speed conditions. Results show that in the worst condition, the maximum value of NO_x reaches to 3.2 g/kWh and soot production in the worst case would be less than 0.45 g/kWh which indicates that, DME appears to be a promising alternative fuel for CI engine operation regarding to future exhaust emissions regulations. Significant reductions in many regulated and unregulated exhaust emissions were observed for DME operation without performing additional engine modifications directed at lowering emissions.

It should be noted that because no experimental emission data was available, exhaust emission with DME and DIESEL fuel are compared relatively based on model simulation.

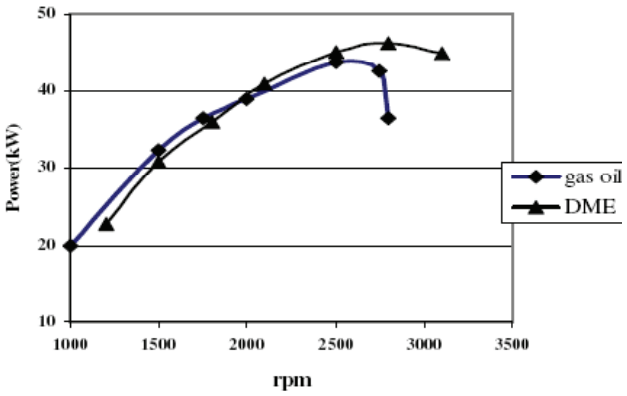

Fig. 8. Comparision of the output power in the case of diesel and DME operation

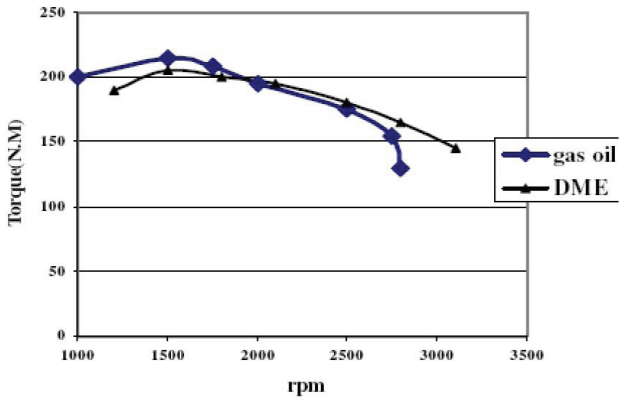

Fig. 9. Comparison of the brake torque in the case of diesel and DME operation

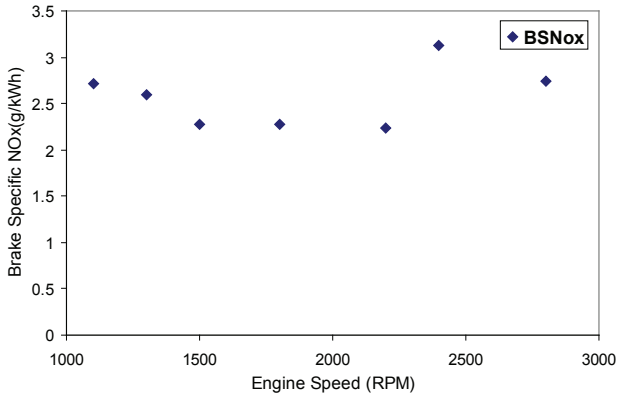

Fig.10. Results of BSNox in different engine speed

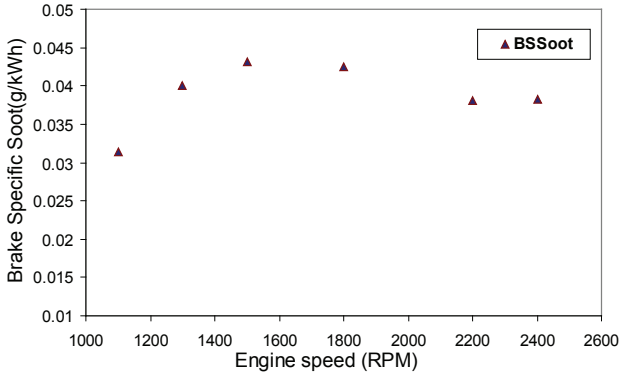

Fig.11. Soot production in different engine speed

7. Conclusion

Results can be summarized as follows:

• Performances and combustion characteristics of a water cooled, 4 stroke naturally aspirated, direct injection diesel engine (Daimler Chrysler motor type, OM314) operating on DME have been experimentally investigated.

• Simulation results shows respectively less than 5% and 3% deviation with experimental results in predicting brake power in low engine speed and high engine speed ranges.

• Considering the accuracy of the simulated results, incylinder pressure and temperature diagram have been compared in the case of maximum brake torque and maximum brake power.

• In the case of maximum torque, incylinder pressure was occurred earlier respect to full load operation and maximum incylinder temperature also decreased in this case.

• In full load operation, the portion of premixed heat released was up to 40% higher than maximum torque case which caused higher rate of pressure rise.

• Results of brake power and related torque in different engine speed have been compared for DME and diesel mode operation. In diesel mode operation, a significant reduction of engine power was occurred in high speed range while in DME mode operation it was not remarkable.

Acknowledgement

The authors would like to thank National Petrochemical Company and the Research and Technology Council of National Petrochemical Company for their kind contributions and support of this project ■

Notation

C1	Constant
S_b	Break up length
d_{inj}	Diameter of nozzle holes
u_a	Local swirl velocity
$\dot{m}_f(t)$	Rate of fuel injection
$u_{i,j}$	Axial velocity of zone [i,j]
n_j	Exponent
u_{ri}	Initial value of radial velocity
[N]	Mole number of N
$u_0(t)$	Initial velocity of the fuel jet
[NO]	Mole number of NO
α	Initial spray angle
q_m	Fuel injection per cycle
ρ_a	Air density
$Q_{z,w}$	Heat transfer from zone to wall
ρ_1	Fuel density
Q	Rate of heat release
τ_z	Ignition delay period of zone
S_{ij}	Axial penetration of zone [i, j]

REFRENCES:

1. Fleisch, T., McCarthy, C., Basu, A., Udovich, C., Charbonneau, P., Slodowske, W., Mikkelsen, S. and McCandless, J., "A New Clean Diesel Technology: Demonstration of ULEV Emissions on a Navistar Diesel Engine Fueled with Dimethyl Ether." SAE Papers, No. 950061, 1995.
2. Sorenson, S. C. and Mikkelsen S. "Performance and Emissions of a DI Diesel Engine Fuelled with Neat Dimethyl Ether." SAE Papers, No. 952754, 1995.
3. Kapus, P. and Cartellieri, W. "ULEV Potential of a DI/TCI Diesel Passenger Car Engine Operated on Dimethyl Ether." SAE Papers, No. 952754, 1995.
4. Kajitani, S., Chen, Z. L., Konno, M. and Rhee, K. T. "Engine Performance and Exhaust Characteristics of Direct Injection Diesel Engine Operated with DME." SAE Papers, No. 972973, 1997.
5. Mikkelsen, S., Hansen, J. and Sorenson, S. "Dimethyl Ether as an Alternate Fuel for Diesel Engines, in Application of Power Train and Fuel Technologies to Meet Emissions Standards, Mardell, J., Parsons, M., Read, J. and Lemon, D., Editor,1996.
6. Gui, B., Wah Leung, C., Xiao, J. and Zhao, L. "Modeling Study on the Combustion and Emissions Characteristics of a Light-Duty Di Diesel Engine Fueled With Dimethyl Ether (Dme), Using a Detailed Chemical Kinetics Mechanism.", SAE Papers, No. 2004-01-1839.
7. Gray, C. and Webster, G. "A Study of Dimethyl Ether (DME) as an Alternative Fuel for Diesel Engine Applications.", Advanced Engine Technology Ltd, TP 13788E.
8. Longbao Z., Hewu W., Deming J. and Zuohua H., "Study of Performance and Combustion Characteristics of a DME-Fueled Light-Duty Direct-Injection Diesel Engine", SAE Papers, No. 1999-01-3669, 1999.
9. Kouremenson D. A., Rakopoulos C. D. and Hountalas D. T. "Multi Zone Combustion Modeling for the Prediction of Pollutants Emissions and Performance of DI Diesel Engines." SAE Papers. No. 970635, 1997.
10. Meng, X., Jiang, Z., Wang, X. and Jiang, D. "Quasi Dimensional Multizone Combustion Model for Direct Injection Engines Fueled with DME." *IMechE*, D01403, 2004.
11. Cui, Y., Deng, K. and Wu, J. "A Direct Injection Diesel Combustion Model for Use in Transient Condition Analysis." Proc. Instn Mech. Engrs, Part D:j. Automobile Engineering, 215, (2001): 995-1004.
12. Turns, S. R., *An Introduction to Combustion, Concepts and Applications*. New York: McGraw-Hill, 1996.
13. Hiroyasu H., Kadota T. and Arai, M. "Development and Use of a Spray Combustion Modeling to Predict Diesel Engine Efficiency and Pollutant Emissions, Part 1: Combustion Modeling." Bull. JSME, 26 :569–575.
14. Jung, D. and Assanis, D. "Multi-Zone DI Diesel Spray Combustion Model for Cycle Simulation Studies of Engine Performance and Emissions." SAE Papers, No. 2001-01-1246, 2001.